Application of Penning Ionization Electron Spectroscopy to Assignments of Electron Spectroscopic Bands of Anthracene

Takashi Kajiwara
Department of Chemistry. Faculty of Science, Toho University, Miyama, Funabashi 274, Japan
Shigeru Masuda, Koichi Ohno, and Yoshiya Harada *
Department of Chemistry, College of Arts and Sciences, The University of Tokyo, Komaba, Meguro, Tokyo 153, Japan

The $He^*(2^3S)$ Penning ionization electron spectrum and He^I u.v. photoelectron spectrum of anthracene were measured. Most observed bands were assigned to various π- and σ-orbitals on the basis of the recently developed concept of exterior electron density (EED), which predicts theoretically the branching ratio of Penning ionization, *i.e.* the relative intensity of Penning ionization spectral bands. A critical comparison between the $He^*(2^3S)$ Penning ionization electron spectrum (PIES) and He^I u.v. photoelectron spectrum (UPS) was also employed for the assignment. Thus, the ionization potentials, ranging from 7 to 16 eV, of 13 σ-orbitals as well as of seven π-orbitals were deduced. The π-orbitals give very strong bands in PIES. The σ-orbitals can be classified into three types, those mainly distributed over adjacent hydrogen atoms, those separately distributed on hydrogen atoms, and those mainly localized on C–C bonds, which give strong, medium, and weak Penning bands, respectively.

U.v. photoelectron spectra (UPS) of anthracene, one of the fundamental aromatic hydrocarbons, have been repeatedly measured and considerable effort has been paid to the assignment of the observed bands.[1–6] This report shows that Penning ionization electron spectroscopy can be effectively applied to this problem.

In contrast to photoionization, the cross-section for Penning ionization is governed by an electron transfer process, which takes place at a quite short inter-particle distance. This enables us to obtain information about the local properties of various molecular orbitals of the target molecule. The He* Penning ionization electron spectra of Na, K, and Hg[7,8] as well as of molecules containing CN groups[9] gave experimental evidence for this electron-transfer mechanism. Further, it was shown that Penning ionization cross-sections of π-electrons are generally larger than those of σ-electrons for conjugated hydrocarbons. This criterion allows us to distinguish the π-band from the σ much more simply and firmly than that based on the perfluoro effect or the asymmetry parameter for the angular distribution of UPS. Thus, all the π-bands of several conjugated molecules have been assigned.[10–12]

In the course of this research, it was recognized that the intensity of a Penning ionization spectral band (Penning band) can be interpreted mainly from the fact that the metastable atom as the ionization source cannot penetrate the target molecule but recoils from the surface of the target. This has led to the study of the outermost molecules of organic films.[13] On the other hand, combined with the aforementioned short-range mechanism of Penning ionization, it also led to the concept of EED (exterior electron density), which could predict semi-quantitatively the relative band intensity of the Penning ionization electron spectrum (PIES). The EED model was successfully applied to the interpretation of the $He^*(2^3S)$ PIES of simple molecules such as CO, H_2O, NH_3, and C_2H_2.[14] Furthermore, it has been shown that theoretical spectra, called EED spectra, can reproduce quite well the main features of the $He^*(2^3S)$ PIES of several conjugated hydrocarbons, especially benzene.[15] In these compounds, the EED spectra predict the difference in intensity not only between the π- and σ-bands but also among various π- or σ-bands. Thus, Penning ionization electron spectroscopy, with the aid of the concept of EED, can be effectively applied to the assignment of all the bands in the UPS of larger aromatic hydrocarbons like anthracene. Veszprémi tried the assignment of all the π-bands and several σ-bands in anthracene applying his revised CNDO/S method.[6] Some of his assignments of σ-bands should be corrected in the light of the present analysis.

Experimental

The transmission-corrected He^I (21.22 eV) UPS and $He^*(2^3S)$(19.82 eV) PIES of anthracene were measured with the apparatus already reported[16] except for the metastable atom source. A high-intensity cold-discharge atom source was constructed for this study. The details will be described elsewhere. The resolution of the electron analyser was 30 meV. High purity anthracene was commercial and was used without further purification. To measure gas-phase spectra, a sample was heated in a Pyrex thimble to *ca.* 120 °C with an electric heater and led into a heated (*ca.* 125 °C) ionization chamber. A liquid nitrogen trap was used to trap sample molecules diffusing out of the ionization chamber in order to protect the electron energy analyser from undesirable contamination. The $1^2\Sigma_g^+$ (VIP 15.579 eV) band of N_2 was used as the internal standard for the calibration of the energies of ejected electrons both in UPS and PIES.

Results and Discussion

Figure 1 shows the observed He^I UPS and $He^*(2^3S)$ PIES of anthracene. Each of 20 bands with ionization potentials < 16 eV was assigned to the corresponding molecular orbital according to an analysis described later in detail. An estimate of the ionization potentials from the PIES bands has been performed on the assumption that the particle–particle interaction term $\delta = 0$. Here δ is defined by the equation $(1/2)mv^2 = E - IP + \delta$, where $(1/2)mv^2$ is the kinetic energy of the ejected electron, E is the excitation energy of the $He^*(2^3S)$ atom, and IP is the vertical ionization potential of the target molecule. With this assumption the abscissae of UPS and PIES in Figure 1 coincide in the ionization potential scale.

The Table shows the vertical ionization potentials obtained from the observed spectra. The calculated ionization potentials, *via* Koopmans' theorem, and the EED values are also shown.

Table. IP values and assignments for anthracene

Band	Orbital	Ionization potential (eV) Calc.	He^{I} UPS	He*PIES	Ne*PIES[a]	EED (%)	Width (eV)
1	π_7 $2b_{2g}$	6.88	7.47	7.43	7.47	3.39	0.25
2	π_6 $2b_{3g}$	8.40	8.51	8.60	8.57	3.10	0.25
3	π_5 $1a_u$	9.33	9.23	9.20	9.23	3.50	0.25
4	π_4 $1b_{2g}$	10.97	10.27	10.25	10.26	3.51	0.25
5	π_3 $2b_{1u}$	11.18	10.4	10.4	10.4	3.53	0.25
6	σ $8a_g$	12.67	11.02	10.9	10.8	2.05	0.30
7	σ $5b_{1g}$	12.94	11.3	(11.3)	(11.2)	0.75	0.30
8	σ $7b_{2u}$	13.37	11.6	11.65	(11.6)	1.49	0.30
9	π_2 $1b_{3g}$	13.39	11.95	12.0	11.9	3.58	0.30
10	σ $6b_{3u}$	14.40	(12.2)	(12.2)	12.3	1.38	0.30
11	σ $7a_g$	14.81	12.7	12.7	(12.6)	1.15	0.30
12	π_1 $1b_{1u}$	14.83	12.95	12.9	12.9	3.52	0.30
13	σ $6b_{2u}$	15.48	13.2	(13.2)	(13.2)	0.68	0.30
14	σ $5b_{3u}$	15.74	13.6	(13.55)	(13.5)	1.42	0.30
15	σ $4b_{1g}$	16.02	14.0	13.8	13.9	1.92	0.30
16	σ $5b_{2u}$	16.83	14.3	14.15		0.74	0.30
17	σ $6a_g$	17.35	14.5	14.6		1.38	0.30
18	σ $4b_{3u}$	16.95	15.0	14.8		2.47	0.30
19	σ $3b_{1g}$	17.44	15.3	15.1		1.23	0.30
20	σ $5a_g$	18.74	15.9	15.7		1.27	0.30

[a] Ref. 12.

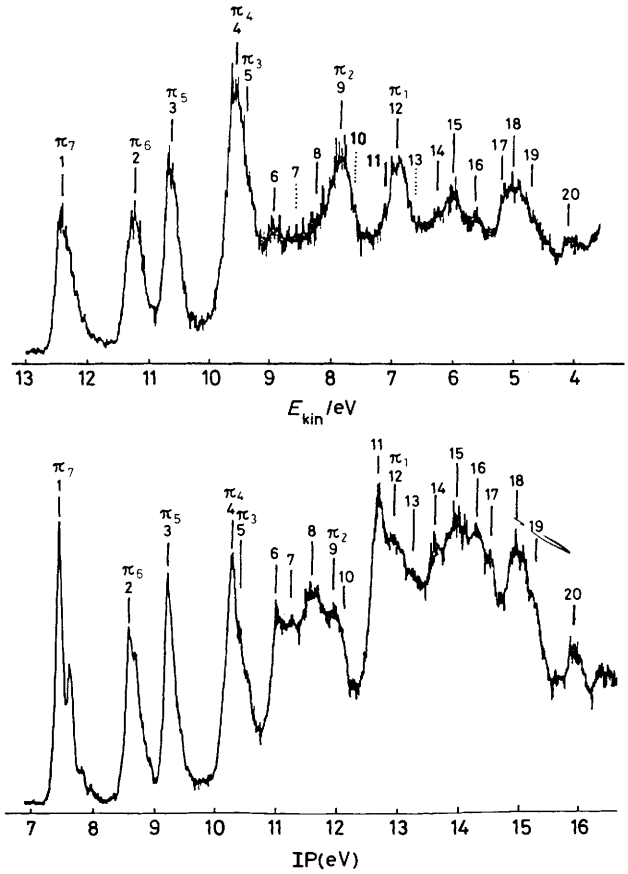

Figure 1. Transmission-corrected He*(2^3S) Penning ionization electron spectrum (PIES, upper) and He^{I} u.v. photoelectron spectrum (UPS, lower) of anthracene

An *ab initio* SCF MO calculation with split-valence-type 4-31G basis functions was performed.[17] D_{2h} symmetry was assumed for the structure of anthracene. The bond lengths and angles were estimated from reported *X*-ray data,[18] by taking a reasonable average so as to produce D_{2h} molecular symmetry. The EED value ρ_i for the *i*th MO (ψ_i) is defined as the probability density of the MO integrated over the region (Ω) accessible for the metastable atom [equation (1)]. For the actual

$$\rho_i(\Omega) = \int_{\Omega} |\psi_i|^2 d\tau \qquad (1)$$

calculation, a region outside a molecular repulsive surface, which was assumed to be a composite of the van der Waals' repulsive surfaces of all the C (van der Waals' radius, r_C 1.7 Å) and H atoms (r_H 1.2 Å) of an anthracene molecule, was adopted as Ω. In order to save computer time, the region distant from this repulsive surface by >0.5 Å was neglected. It has been verified that this approximation introduces no serious error because the probability density decreases quite rapidly as the distance from the molecule increases.[15] Discussions about the computational method and the estimate of the errors involved in the various approximations have been given in refs. 14 and 15.

The assignments of the bands have been performed by means of the following two guides. (i) The integrated intensity of a band in PIES should be roughly proportional to the calculated value of EED. (ii) Each band in UPS shows a 1:1 correspondence with a band in PIES. As the Table shows, the differences in ionization potentials deduced from UPS and PIES are $<$*ca.* 0.2 eV, although the intensities are very different owing to the different ionization mechanisms.

Generally speaking, the maximum position, width, and shape of a PIES band are not determined mainly by the Franck–Condon factor in contrast to the case of UPS. Hotop and Niehaus showed that the interaction potential curve for the metastable projectile and the target molecule [V*(R)] plays an important role in these properties of the band.[8] When the interaction is attractive and rather strong, a large shift and considerable broadening of the band occur.[7] For instance, the band width reaches 735 meV in the He*(2^3S)–Na system[7] and >2 eV in the He*(2^3S)–H system.[8] In these cases, the spatial overlap of the vacant (or occupied) orbital of the projectile and the occupied (or vacant) orbitals of the target is rather large and

some sort of bonding interaction occurs when the two particles approach. In contrast to these cases, however, the valence orbitals of condensed aromatic hydrocarbons are usually delocalized and the above mechanism for the shift and broadening is expected not to operate. Indeed, in the case of benzene, the magnitude of the shift was found to be <0.1 eV, and no significant broadening of the PIES bands was observed compared with the UPS bands.[14]

The positions of bands 7, 10, and 13 in the He*(2^3S) PIES seem to be rather ambiguous (as indicated by dotted bars in Figure 1), but these bands have also been observed in the Ne*($^3P_2$) PIES as shoulders.[12] For comparison purposes, the band positions estimated from the latter spectrum (Figure 3 in ref. 12) are included in the Table. The assignments of the bands on the basis of the above discussion are also given in the Table. These bands can be classified as follows.

(a) The first type are those observed as distinct bands both in UPS and PIES. The relative intensities of the PIES bands in this group show a semi-quantitative agreement with the relative EED values calculated. All π-bands (1—5, 9, and 12) and three σ-bands (6, 15, and 18) are included in this group.

(b) The second group are observed either in UPS or in PIES. In this case, the observed Penning band intensities conform to the calculated values of EED. This group contains bands 8, 11, 14, 16, and 20.

(c) The final group have such small intensity that they appear only as weak bands or shoulders both in UPS and PIES. Their positions were determined so that the calculated EED spectrum might best reproduce the observed PIES. Their intensities do not contradict the calculated values of EED as illustrated in the EED spectrum (see below). Bands 7, 10, 13, 17, and 19 belong to this group.

Bands 6(σ, $8a_g$), 15(σ, $4b_{1g}$), and 18(σ, $4b_{3u}$) have EED values considerably larger than the other σ-bands. The latter two bands are observed in PIES nearly as distinctly as the π-bands, and the corresponding bands in UPS are also quite evident. They assist in the assignment of other bands. Band 6 follows bands 15 and 18 in the magnitude of EED and also serves as a marker for the assignment, although it is not so obvious in PIES, appearing in the tail of the strong $\pi_3 + \pi_4$ band.

Band 11 is quite distinct in UPS, but is weak in PIES as predicted by the rather small value of EED. In contrast to this, band 17 is almost missing in UPS, but is observed as a shoulder in PIES. These bands are also examples of the usefulness of the EED model.

The present assignments are not contrary to the order of the calculated ionization potentials except for bands 17 and 18. Von Niessen *et al.* showed, by their elaborate calculation including the correlation and reorganization effects, that Koopmans' theorem gives the correct order in the case of benzene,[18] in which the correlation and reorganization effects make roughly the same contribution to the energies of various molecular orbitals and thus keep the order of the SCF energy unchanged. It may be fairly reasonable to expect a similar situation for most occupied valence levels of the anthracene molecule, though, of course, we admit that the validity of Koopmans' theorem must be carefully examined for each level of an individual molecule. Von Niessen, Cederbaum, and their co-workers demonstrated many cases where Koopmans' theorem fails.[19–23]

Figure 2 shows the EED spectrum composed of Gaussian-shaped bands with areas proportional to the calculated values of EED. The band-widths and positions were approximately adjusted to the experimental values shown in the Table. The relative intensities of the π_7 (1), π_6 (2), π_5 (3), and $\pi_4 + \pi_3$ (4 + 5) bands in PIES are semiquantitatively reproduced by the theoretical spectrum. Although the overlap of bands and the contribution from scattered electrons to the experimental PIES make the quantitative comparison a little difficult at the lower

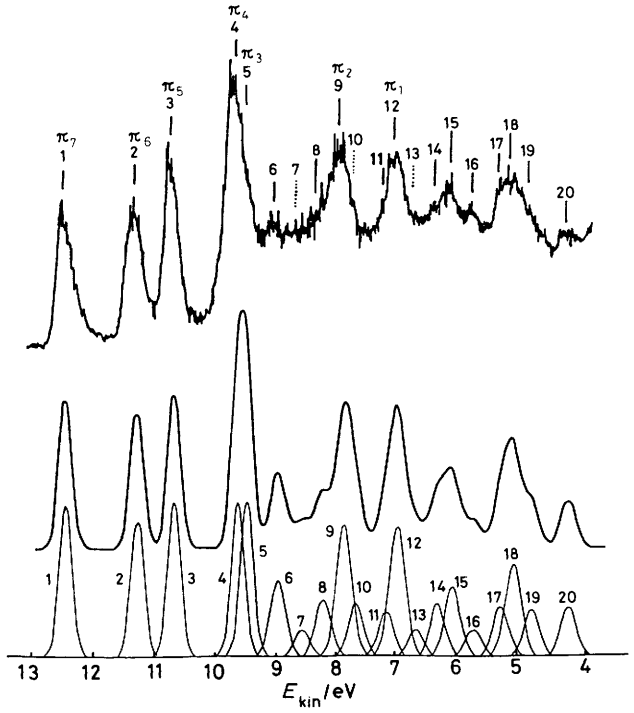

Figure 2. Penning ionization electron spectra of anthracene. Upper: observed spectrum also shown in Figure 1. Lower: calculated spectrum on the basis of the EED model. The detailed procedure for obtaining the EED spectrum is described in the text

electron-energy region, the overall characteristics of PIES are well reproduced by the EED spectrum. Therefore, our assignments of the bands in UPS and PIES are considered to be reasonable.

The above assignments of the π-bands are in agreement with those of the previous UPS studies, in which some lower lying π-bands were assigned on the basis of simple or semi-empirical MO calculations.[1–5] Veszprémi[6] tried to assign all the π-bands and the lowest six σ-bands in UPS, applying his revised CNDO/S calculation. Although his assignments of the π-bands agree with ours, those of the σ-bands are different; he related bands 6—8 to the b_{1g}, a_g, and b_{2u} σ-orbitals and also picked up three σ bands between the π_2 and π_1 bands. We believe that our assignments based on the EED analysis as well as on the *ab initio* MO calculation are more reliable. For example, the lowest σ-band is assigned to the $8a_g$ orbital and not to $5b_{1g}$, because the $8a_g$ orbital with a larger EED value should give a stronger band in PIES (see Figure 2).

Finally, we interpret our assignment from the standpoint of the stereochemical characteristics of orbitals with the aid of the contour lines for electron density shown in Figure 3. It is obvious that all the π-orbitals extend out of the repulsive surface of the molecule to give large values of EED. It must be noted here that the correct order of the EED values of various π-orbitals must be predicted not from qualitative geometrical characteristics of orbitals such as the number of nodal planes but from the quantitative results of the EED calculation. In Figure 3, the $4b_{3u}$ (18) orbital, giving rise to the strong PIES band 18, has a distinctive electron density distribution that extends over the three adjacent C–H bonds on the upper and lower sides of the molecule. The $8a_g$ (6) and $4b_{1g}$ (15) orbitals have similar electron density distributions extending over adjacent C–H bonds, thus giving rather strong PIES bands. In contrast, the $5b_{1g}$ (7), $6b_{2u}$ (13), and $5b_{2u}$ (16) orbitals, corresponding to weak PIES bands, have electron density

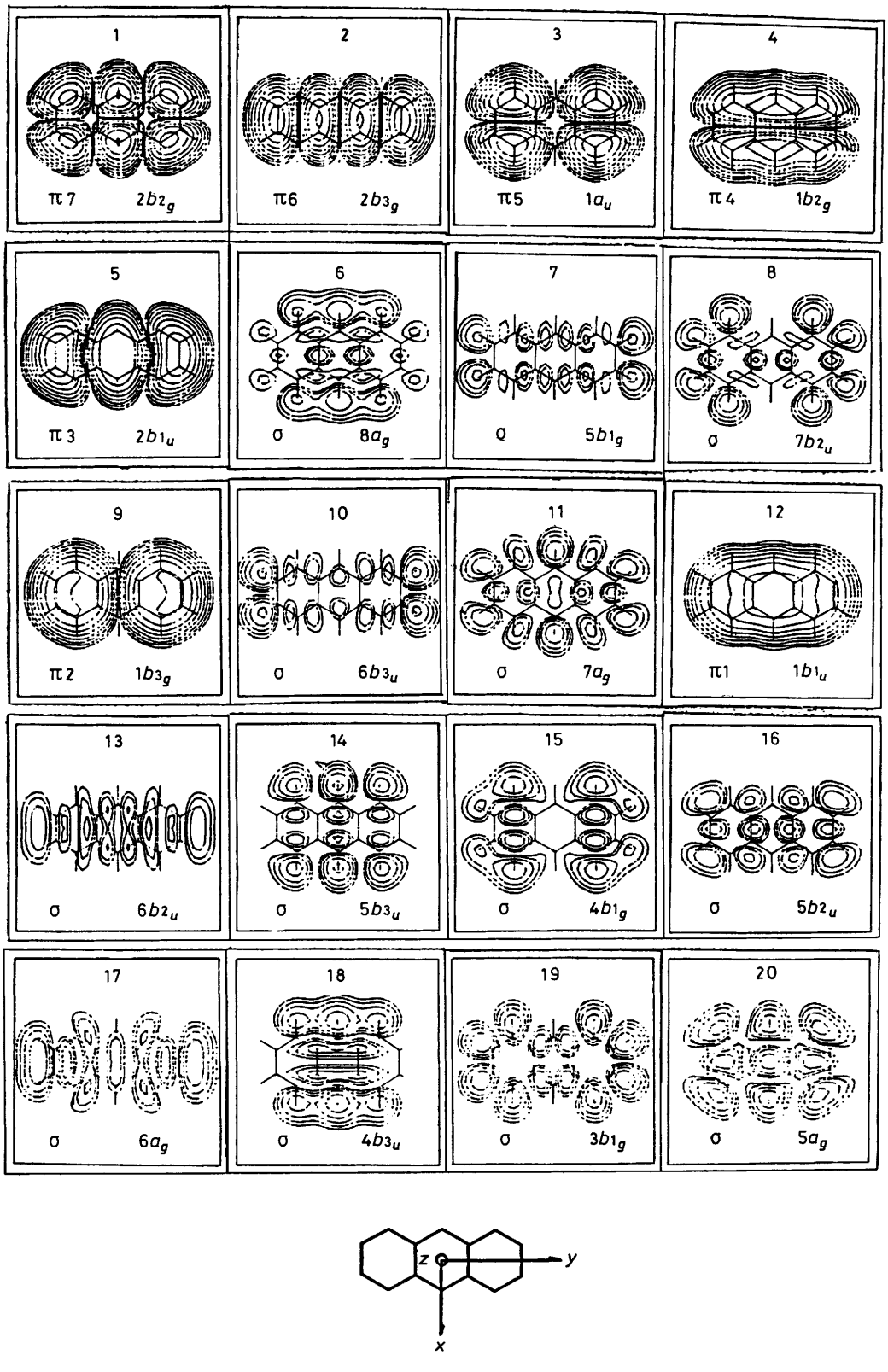

Figure 3. Contour lines of the electron density of various molecular orbitals of anthracene on a plane 1.7 Å above the molecular plane. The density of the *n*th line from the outside is $2^n \times 10^{-6}$ au^{-3}. The number of each map corresponds to that of each band in the UPS and PIES shown in Figure 1

distributions localized on C–C bonds and mostly confined in the interior of the repulsive molecular surface.

The classification of the orbitals is briefly summarized as follows: (a) π-orbitals, very strong bands in PIES (1—5, 9, and 12); (b) σ-orbitals, mainly distributed over adjacent hydrogen atoms, strong bands (6, 15, and 18); (c) σ-orbitals, separately distributed on hydrogen atoms, medium bands (8, 10, 11, 14, 17, 19, and 20); (d) σ-orbitals, mainly localized on C–C bonds, weak bands (7, 13, and 16).

This kind of classification, when combined with the concept of EED, can be a quite effective aid for the assignment of PIES bands.

In the present study, the use of He* as the excitation source, instead of Ne* as in the former work,[12] enlarged the observable region of the ionization band up to IP 16 eV. It has been shown that the concept of EED greatly helps to assign the observed bands. The present method can be applied to many other conjugated hydrocarbons and will considerably advance the interpretation of the PIES and UPS of those molecules.

Acknowledgements

We thank Mr. K. Imai for help in experiments and Mr. T. Ishida for help in calculations. Thanks are also due to Professor H. Hotop and Dr. M.-W. Ruf, Universität Kaiserslautern, for informing us of the details of their cold-discharge metastable atom source.

References

1 P. A. Clark. F. Brogli, and E. Heilbronner, *Helv. Chim. Acta*, 1972, **55**, 1415.
2 R. Boschi, E. Clar, and W. Schmidt, *J. Chem. Phys.*, 1974, **60**, 4406.
3 W. Schmidt, *J. Chem. Phys.*, 1977, **66**, 828.
4 D. G. Streets and T. A. Williams, *J. Electron Spectrosc. Relat. Phenom.*, 1974, **3**, 71.
5 N. S. Hush, A. S. Cheung, and P. R. Hilton, *J. Electron Spectrosc. Relat. Phenom.*, 1975, **7**, 385.
6 T. Veszprėmi, *Chem. Phys. Lett.*, 1982, **88**, 325.
7 H. Hotop and A. Niehaus, *Z. Phys.*, 1970, **238**, 452.
8 A. Niehaus, *Ber. Bunsenges. Phys. Chem.*, 1973, **77**, 632.
9 V. Čermák and A. J. Yencha, *J. Electron Spectrosc. Relat. Phenom.*, 1976, **8**, 109.
10 T. Munakata, K. Kuchitsu, and Y. Harada, *Chem. Phys. Lett.*, 1979, **64**, 409.
11 T. Munakata, K. Kuchitsu, and Y. Harada, *J. Electron Spectrosc. Relat. Phenom.*, 1980, **20**, 235.
12 T. Munakata, K. Ohno, Y. Harada, and K. Kuchitsu, *Chem. Phys. Lett.*, 1981, **83**, 243.
13 T. Munakata, K. Ohno, and Y. Harada, *J. Chem. Phys.*, 1980, **72**, 2880; H. Kubota, T. Munakata, T. Hirooka, K. Kuchitsu, and Y. Harada, *Chem. Phys. Lett.*, 1980, **74**, 409; Y. Harada, H. Ozaki, K. Ohno, and T. Kajiwara, *Surface Sci.*, 1984, **147**, 356.
14 K. Ohno, H. Mutoh, and Y. Harada, *J. Am. Chem. Soc.*, 1983, **105**, 4555.
15 K. Ohno, S. Matsumoto, and Y. Harada, *J. Chem. Phys.*, 1984, **81**, 4447.
16 Y. Harada, K. Ohno, and H. Mutoh, *J. Chem. Phys.*, 1983, **79**, 3251.
17 R. Ditchfield, W. J. Hehre, and J. A. Pople, *J. Chem. Phys.*, 1971, **54**, 724; N. Kosugi, Program GSCF NEW V, Program Library, The Computer Center, The University of Tokyo, 1984.
18 D. W. J. Cruickshank, *Acta Crystallogr.*, 1956, **9**, 915.
19 W. von Niessen, L. S. Cederbaum, and W. P. Kraemer, *J. Chem. Phys.*, 1976, **65**, 1378.
20 W. von Niessen, G. H. F. Diercksen, and L. S. Cederbaum, *J. Chem. Phys.*, 1977, **67**, 4124.
21 W. von Niessen, W. P. Kraemer, and J. Schirmer, *J. Chem. Soc., Faraday Trans. 2*, 1981, **77**, 1461.
22 W. von Niessen, W. Domcke, L. S. Cederbaum, and J. Schirmer, *J. Chem. Soc., Faraday Trans. 2*, 1980, **74**, 1550.
23 W. von Niessen, W. P. Kraemer, and G. H. F. Diercksen, *Chem. Phys.*, 1979, **41**, 113.

Received 2nd March 1987; *Paper* 7/692